DOI 10.52209/2706-977X_2024_2_44 IRSTI 55.03.14 UDC 621.01

Strength analysis by the Finite Element Method (FEM) of a modular line

Marcinkiewicz J. *, Spadło M., Staszak Ż.
Poznan University of Technology, Poznan, Poland
*corresponding author

Annotation. The aim of the work is the strength analysis of structural elements of a modular line. Within the subject, an assessment of the structural strength state was made using the finite element method. For the purpose of the work, the following computational models were developed: the load-bearing frame of a charging hopper, the load-bearing frame of a screen as well as the load-bearing structure of wheels. The problem of load transfer between components occurring in mutual contact was discussed. Multi-variant strength calculations were performed later and stress patterns were determined for all the most important operating cases. The final stage of the work was the verification of the adopted design assumptions in terms of stress with the results obtained during the tests.

Key words: finite element method, FEM, strength analyse

Introduction

The first information on application of finite elements was available in the mid-60s in 20th c. At the beginning they were used in mechanics and the machine and construction facilities' design process. However, the complicated boundary conditions made formulating issues concerning a mathematical analysis impossible. Mathematics development allowed of changing the problem description from the analytical to algebraic form and of applying this solution to issues related to mechanics [1].

The Finite Element Method (FEM) allows of physical calculations based on the discretisation of an area with a finite number of elements averaging the body physical state. The finite element is understood as the sub-area of the discretised continuum. Its dimension is finite and its shape is simpler than the geometric shape of the examined object [2, 7]. The particular elements should be small in size so that the base functions approximated in them could be approximated by means of polynomials, but they must differ from zero, whereas the base elements should be simple solids while discretising space or simple figures while discretising surfaces [1-3, 33, 35-37].

The selection of points for analysis, called nodes, aims at determining the input function conditions of compatibility and equilibrium, whereas each of the nodes is characterised by an appropriate number of degrees of freedom. There are six degrees of freedom for solid elements, hence a three-dimensional model, while for flat elements the number of degrees of freedom is three and a two-dimensional model is created. The accuracy of the solution depends on the shape function, i.e. the accuracy of the approximation of physical quantities inside the element [2-4, 32, 38-40].

The shape functions should meet the following assumptions: there is no need for continuity of derivatives between the elements, the matrix of the whole system is created on the basis of the matrix of elements. This allows the basic system of equations to be solved and on the basis of determined nodal parameters derivative functions are calculated [1, 5].

Computer programmes making FEM calculations consist in preparing the calculation process, building and solving an appropriate system of equations which can be presented in the form of print-outs or graphs [3-4].

The finite element method is used by Hou et al. [14] to analyse the helical gear mesh stiffness. Tan, et al. [15], uses the FEM to locate mechanical damage, whereas Hakula and Lakksonen [16] to analyse perforated material damage. The finite element method is also applied in the shipbuilding industry, e.g. when evaluating the thermal properties of fire doors on a ship [17]. The described method does not only concern steel materials, but can also be used for the analysis of building materials in order to assess their strength [18] and for the analysis of reinforced concrete elements [19-20] used during the construction of large buildings.

The finite element method is used much more often while designing machines and equipment. Azarinfar and Aghaebrahimi [21] applied it to calculate the disk rotor using permanent magnets with cross-flow. Ścieszka and Żołnierz [22] used the finite element method to calculate the effect of the hoisting machine disk brake design on its thermal-elastic instability. This method is also used during the cracking analysis of machine elements [23,25,34,41] and issues related to the contact of machine elements [24,31,35,42].

The finite element method used for the stress analysis requires a lot of work on model preparation and synthesis of results [43]. It is now an integral part of the design process [44]. It is applied in the stress analysis in complex mechanical systems [45-46]. Due to the FEM, it is possible to examine the strength of the structure, its dynamics, stresses, displacements, kinematics and statics, simulate deflections and check the flow of liquids and heat [47]. Apart from its application in many fields of technology, it is also used in bioengineering and medicine [6-8].

1. Purpose and Scope of work

The investigated constructions were designed as space frame systems which are the basic load-bearing system for the charging hopper (Fig. 1) and the vibrating screen (Fig. 2). Due to the nature of input functions, the adopted construction solutions were selected in order to ensure full structure stability even in unstable foundation conditions on demanding ground therefore most of the structural joints are designed as welded joints. In the structure of both frame structures, as the basic construction elements there were used I-section stringers connected with crossbars and reinforced columns, which were reinforced with braces at critical points. For strength reasons, the number of bolted joints is limited to the minimum to maintain the proper functionality of the designed structures [9-10].

Strength considerations also regarded a driving unit, additional equipment of the discussed frame systems (Fig. 3) which is an innovative solution on the market and can also be used as a bogie for transporting heavy and bulky materials. The construction supported by eight wheels in twin subsystems was designed to guarantee the mobility of the newly designed technological line. In the construction structure, a load-bearing element in the form of a lateral axis and articulated bogies mounted at its ends can be distinguished.

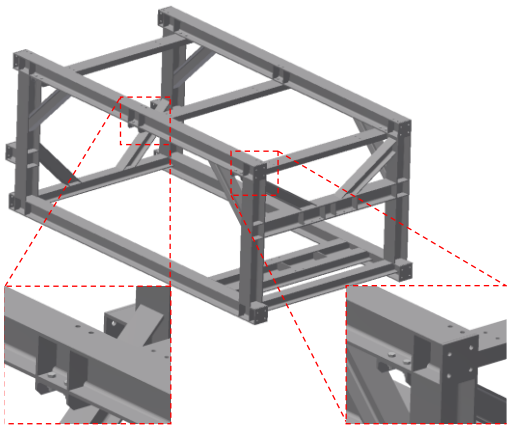

Fig. 1. - Charging hopper frame

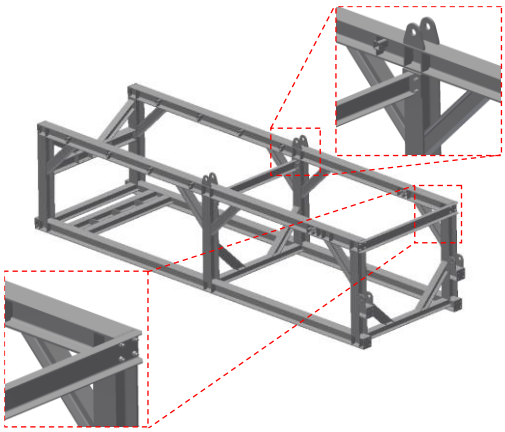

Fig. 2. - Vibrating screen frame

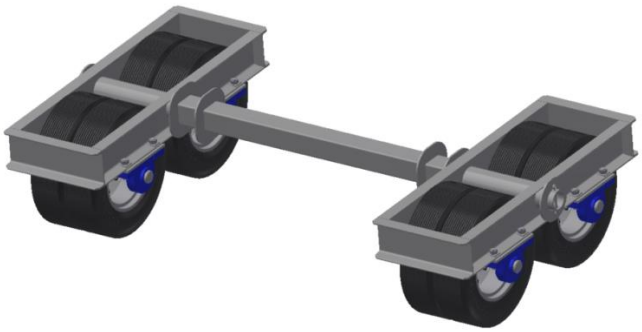

Fig. 3. - Driving unit model – top view

Only selected system components were analysed in the work. Commercial components and those which are not affected by high amplitude loads, i.e. crucial from the strength point of view, were omitted in the analysis.

For the main structural elements in the design, unalloyed structural steel, hot-rolled S355 J0, for which the yield stress is 355 MPa, was selected. It is killed steel of a ferritic-perlite structure in delivery condition, usually used in the construction of sensitive machine and equipment elements [11].

2. Strength analyses using the fem and the computational model construction

For the load-bearing frame, intermediate frames and all other non-integral elements, the standard rules for the conclusion of the material stress were applied, based on the hypothesis of the highest energy of effort state (Huber-Misses Hencky hypothesis) [13]. The following assumption was made (1):

$$\boldsymbol{k_{dop}} \leq \frac{Re}{x}, \tag{1}$$

where:
Re - material yield stress (355 MPa),
x - safety factor adopted arbitrarily.

On the basis of the experiments of the research team performing the calculations, the following safety factor values were adopted:

x_{native} = 1.2 - for a native material,

x_{joints} = 1.6 – for joints.

Hence:

$k_{dop\ native}$ = 295 MPa,

$k_{dop\ joints}$ = 221 MPa.

In order to construct the computational model, there were used techniques facilitating the imposition of the finite element mesh, while maintaining a high reflection of the geometric form of the analysed structure. The first step in the process was to simplify the virtual model.

In the context of load-bearing frames, the simplification consisted in replacing the volumetric model with the surface one, and as it was decided to use two-dimensional meshes, inclinations and slight rounding radii were removed. These elements in the virtual space have a certain height and width, while the thickness is stored in the computer memory as a single scalar size. Such an approach is appropriate for modelling fragments of slender, long, extensive structures whose thickness does not exceed 10% of their length or width [12]. Usually these are sheet metal elements as well as sections with open and closed cross-sections.

This process was carried out by the use of a function which automatically searches the central surface. This results in deactivating the view of elements containing finite volume and displaying only generated surfaces.

For the model prepared in this way it is possible to superimpose two-dimensional meshes which will help to perform calculations (Fig. 4 and 5). Additionally, it is possible to change quickly the thickness of T-profiles, structural channels, angles and sheet metal by changing one parameter, without the necessity to update the finite element meshes, which also increases the efficiency of the considerations.

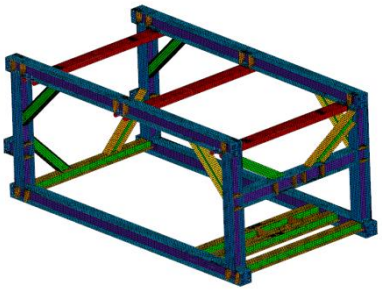

Fig. 4. - Mesh of two-dimensional elements of the charging hopper frame

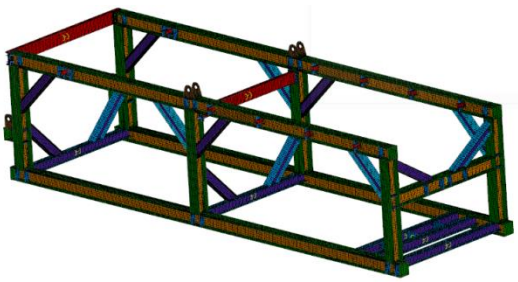

Fig. 5. - Mesh of two-dimensional elements of vibrating screen load-bearing frame

In the both analysed cases (Fig. 4 and 5), the second order (parabolic) mesh was used - it consists in the superimposition of additional calculation nodes between nodes located in the vertices of geometric figures, which increases the accuracy of calculations. The triangular mesh was used in places where the degree of geometric complexity of a structural element was large and the superimposition of the square mesh was impossible or significantly impeded by the impossibility of superimposing the square element without the introduction of the so-called "deformations", which consisted in the appearance of open angles between the sides of the quadrilateral with a value equal or exceeding 180 degrees. Then it is impossible to properly determine the stiffness matrix of the element.

During the development of the computational model, the geometry was simplified by removing minor rounding, undercutting and chamfering. However, holes were left which will then be used to model the bolted joints.

Superimposing three-dimensional meshes was performed using tools for automatic filling of selected volumes with finite elements. For the purpose of the discretisation, three-dimensional second-order pyramidal elements with additional nodes between the vertices and medium-density meshes were applied, whereas for the bearing frame a low-density mesh was used (Fig. 6).

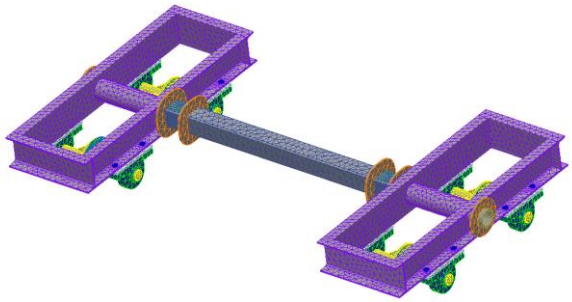

Fig. 6. - Mesh of two-dimensional elements of vibrating screen load-bearing frame

The analyses took into account the presence of bolts and their interactions with structural elements of the system. In case of the bolt-nut combination, the bolt head and nut were modelled using one-dimensional elements of RBE2 type. These elements are characterised by infinite stiffness, i.e. not susceptible to deformation. These elements were distributed using the so-called "spider" technique, i.e. a node, called the central node, was placed in the axis of the bolt, with which all nodes lying on the circles of holes through which the bolts are installed were connected via RBE2.

The core of the bolt itself was modelled from CBAR type elements, i.e. beam elements transferring tensile forces and bending moments. These elements were placed between the central nodes. This way of implementing bolted joints allows of reading the forces' values occurring in the joints during operation without going into details of stress patterns, displacements or deflections. At the same time, bolt stiffness (by using CBAR) is reflected in the correct way; hence the whole structure will be reliable.

The so-called "preload", i.e. the initial tension resulting from tightening the bolts to a given torque, is introduced in all bolt joints. The value of the preload was determined depending on the bolt size and strength class.

All significant force interactions, i.e. gravity and external input functions were taken into account to develop boundary conditions of the analyses (loads and supports).

For load-bearing frames, loads were applied over the entire length of the main beams. The load value is 100 kN, which corresponds to an application of 10 tons of mass. The degrees of freedom were reduced so that the possibility of longitudinal movement with all the nodes belonging to the lower beams was restrained, as shown in Figure 7.

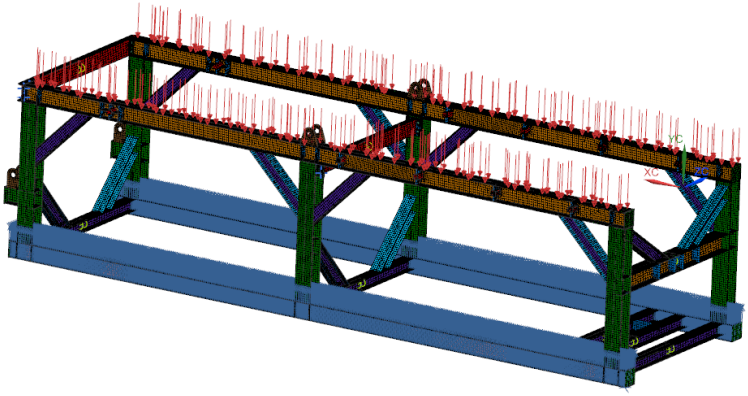

Fig. 7. - The method of modelling the boundary conditions of the analysis on the example of a vibrating screen frame. The red arrows illustrate the forces, whereas the blue arrows illustrate the reduced degrees of freedom

Figures 7 and 8 show the layout of boundary conditions for the analysed load cases. In such a state it was assumed that the main load of the tested structures is a vertical force Fy (10 t) generated by the mass of installed devices and gravitational acceleration g. The distribution of forces affecting the structural elements was carried out in accordance with the distribution resulting from the construction of the installed devices.

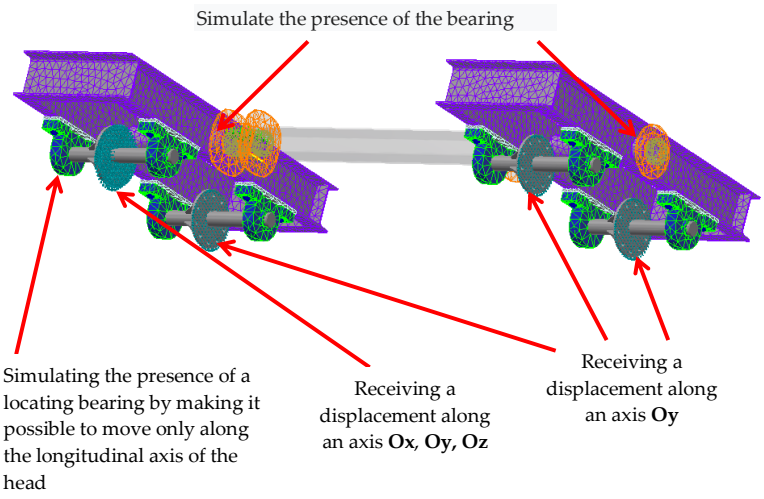

Fig. 8. - The reduced degrees of freedom for the computational model of a driving unit

Then, strength analyses were carried out for: the charging hopper frame, the vibrating screen frame and the driving unit.

For the frame of the charging hopper, the stress map H-M-H is shown in Fig. 9 because only these stresses are relevant for the accepted criteria, whereas Fig. 10 shows its displacements.

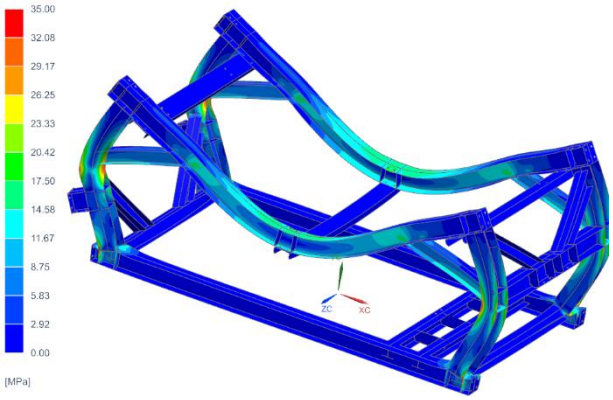

Fig. 9. - The stress map H-M-H, for the charging hopper frame (load 10t) – displacements in scale 200:1 – general view unit

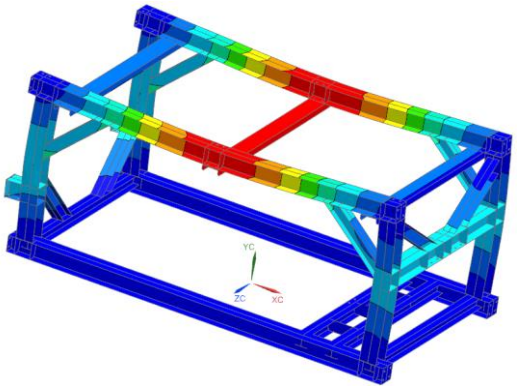

Fig. 10. - Displacement map, for the charging hopper frame (load 10t) – displacements in scale 100:1 – general view

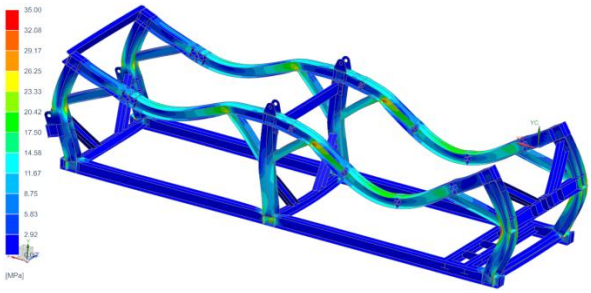

Fig. 11. - The stress map H-M-H, for the frame of the vibrating screen (load 10t) – displacements in scale 1000:1 – general view

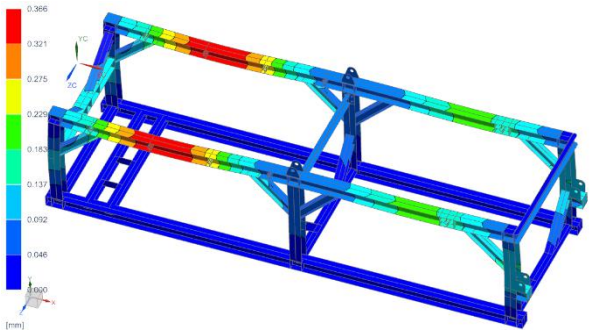

Fig. 12. - The displacement map for the Frome of the vibrating screen (load10t) – displacements in scale 100:1 – general view

The last stage was to present the stress map H-M-H for the frame of the driving unit (Fig. 13) and the map of its displacements (Fig. 14).

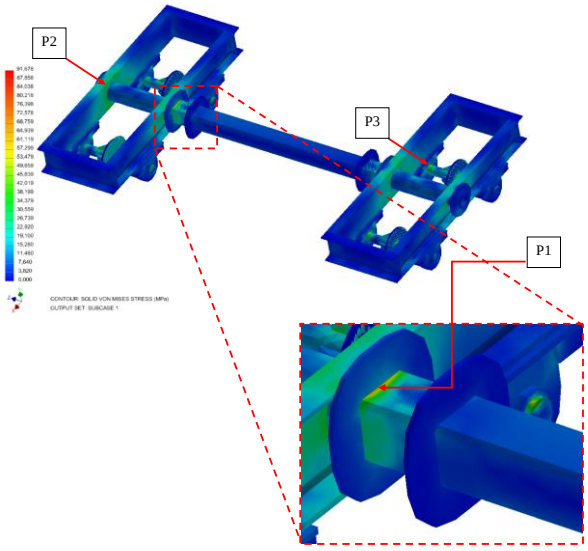

Fig. 13. - The stress map H-M-H, for the frame of the driving unit (load 10t) – top view

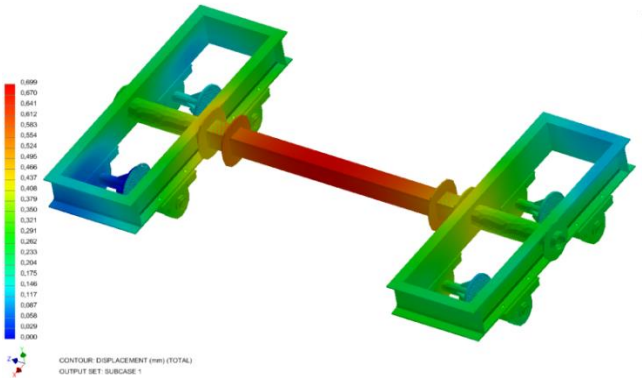

Fig. 14. - Displacements of mesh nods for the frame of the driving unit

3. Fatigue analysis

For the purpose of estimating the fatigue durability of the S355 steel structure, the Goodman-Smith diagram was utilized. Among the considered cases, the driving unit frame was taken into consideration. For the analyzed scenario, the stress amplitude was determined from the difference between the stress values obtained for the static loading case and the maximum operational loading case. For the construction of the computational model in the analyzed scenario, asymmetric loads were assumed in the form of unloading on one side. In this particular case, one side of the frame is completely unloaded (reaction forces equal zero), and the other side is maximally loaded.

Based on the analysis results for the examined points, average stress values were determined. In Fig. 13, the locations where maximum stress values were read for the mentioned two load cases are shown. The determined stress amplitudes and averages are plotted on the Goodman-Smith diagram for S355JO steel (Fig. 15).

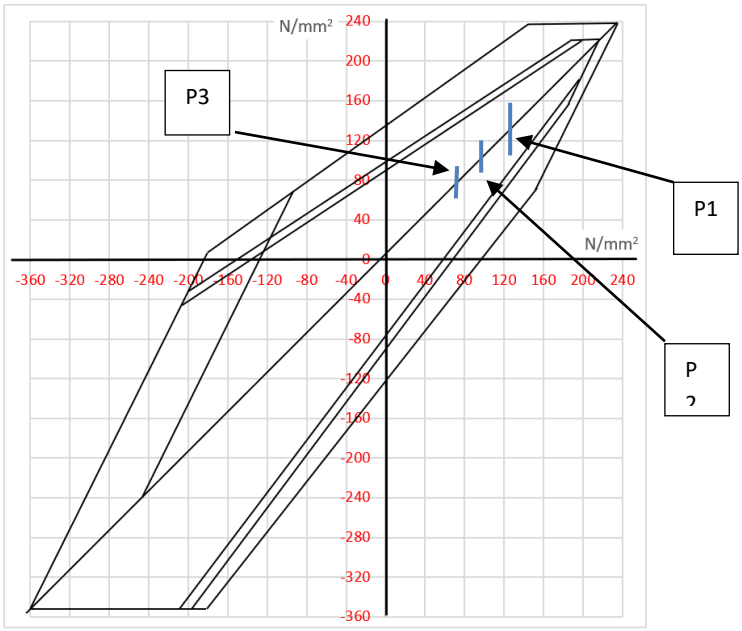

Fig. 15. - The Smith chart for S355JO steel, with selected mean and amplitude stresses plotted at measurement points for the frame of the driving unit

Conclusions

According to the above results, it is concluded that the device load-bearing structure meets the strength criteria [28]:

$k_{dop\ native}$ = 295 MPa,

$k_{dop\ joints}$ = 221 MPa .

The applied method is consistent with the method adopted by Truty et al. [26] in their work on the strength of the press adaptation table, Selech et al. [27] and Marcinkiewicz et al. [29, 30] in their work presenting a machine for laying drainage hoses.

In the analysed model, no points were observed where the stresses would exceed a value greater than 20% of the joint's permissible stresses. The analyzed structure is characterised by high stiffness and is not susceptible to deflections, which makes it possible to reduce its weight by implementing beams, sheet metal and profiles with smaller cross-sections and strength indicators. The material used is appropriate, and the von Misses stress values obtained during simulation tests are lower than the Re value. The risk of plasticization is very low. There is no possibility of replacing the material with another one with a lower yield strength. In order to verify the above calculations, it is necessary to make a prototype and perform tests with the use of strain gauges to validate computer calculations of the structure.

The forces in the bolts connecting the individual sections are low and reach a value of at most several percent of their load capacity. It has been observed that some of the bolts transmit compressive forces, which should be interpreted as the fact that they take over the compressive loads between the structural elements being in contact with each other.

The designed model is characterised by high load capacity, if the prototype and later serial production are made according to the above recommendations; the risk of malfunctioning due to improper stress is minimal.

In the context of fatigue analysis, it was not observed that in the three analyzed points (P1, P2 and P3), the lines representing the stress range went beyond the area of the permanent fatigue limit for the Goodman-Smith chart. This means that there is a possibility of long-term cyclic loading of the tested object without the risk of fatigue

cracks. In the context of fatigue analysis, it was not observed that in the three analyzed points (P1, P2 and P3) the lines representing the stress range went beyond the area of the permanent fatigue limit for the Goodman-Smith chart. This means that it is possible to load the tested object for a long time, cyclically, without the risk of fatigue cracks.

References

[1] Łodygowski T., Kąkol W.: Metoda elementów skończonych w wybranych zagadnieniach mechaniki konstrukcji inżynierskich. Wyd. PP, Poznań, 1994, 1-2.
[2] Zienkiewicz O. C.: Metoda elementów skończonych. Arkady, Warszawa, 1972, 63-84.
[3] Balonek K., Gozdur S.: Wprowadzenie do Metody Elementu Skończonego. Wydział Fizyki i Informatyki Stosowanej, AGH, Kraków, Poland [dostęp: 10 stycznia 2020]. Dostępny w internecie: http://fatcat.ftj.agh.edu.pl/~i6balone/MES.Pdf.
[4] Fortuna Z., Macukow B., Wąsowski J.: Metody numeryczne. Wyd. Naukowo-Techniczne, Warszawa, 1993.
[5] Lohrengel A., Kramarczyk W., Kruk R., Twardoch K., Wieczorek A.: Modelowanie zjawisk dynamicznych w przekładniach zębatych, z wykorzystaniem metody elementów sztywnych. Górnictwo i geologia, 2011, 6(3), 115-126.
[6] Kruszewski J., Sawiak S., Wittbridt E.: Metoda sztywnych elementów skończonych w dynamice konstrukcji. Wyd. Naukowo-Techniczne, Warszawa, 1999.
[7] Gilewski W.: Some considerations on the finite element method. Sci. Rev. Eng. Eb=nv. Sci. 62, 2013, 502-510.
[8] Dobosz A, Panek H., Dobosz K.: Implementation of Finite Elements Method in Evaluatiom of Stresses in Dental Hard Tissues. Dent. Med. Probl., 2005, 42, 4, 651-655.
[9] Moss R., Basic M. : Pressure Vessel Design Manual. 4th Edition. Butterworth-Heinemann, 2012.
[10] Niemi E., Marquis G.: Introduction to the Structrual Stress Approach to Fatigue Analysis of Plate Structures, Lappeenranta University of Technology.
[11] Polska norma PN-EN 1561:2012 „Żeliwo szare".
[12] Tabor A., Zarębski K., Putyra P.: Wpływ temperatury na właściwości mechaniczne sferoidalnego żeliwa austenitycznego o zawartości niklu 20%. Archiwum Odlewnictwa, 2006, Rocznik 6, Nr 21(1/2).
[13] Niezgodziński M.E., Niezgodziński T.: Wzory wykresy i tablice wytrzymałościowe. WNT, Warszawa, 2004.
[14] Hou, S., Wei, J., Zhang, A., Zhang, C., Yan, J., Wang, C.: A Novel Comprehensive Method for Modeling and Analysis of Mesh Stiffness of Helical Gear. Applied Sciences, 2020, 10(19), 6695.
[15] Tan, X., Chen, W., Wang, L., Yang, J.: Analysis of Local Damages Effect on Mechanical Responses of Underwater Shield Tunnel via Field Testing and Numerical Simulation. Applied Sciences, 2020, 10(18), 6575.
[16] Hakula, H., Laaksonen, M. Frequency response analysis of perforated shells with uncertain materials and damage. Applied Sciences, 2019, 9(24), 5299.
[17] D'Amore, G. K. O., Mauro, F., Marinò, A., Caniato, M., Kašpar, J.: Towards the use of novel materials in shipbuilding: assessing thermal performances of fire-doors by self-consistent numerical modelling. Applied Sciences, 2020, 10(17), 5736.
[18] Invernizzi, S., Lacidogna, G., Carpinteri, A.: Numerical models for the assessment of historical masonry structures and materials, monitored by acoustic emission. Applied Sciences, 2016, 6(4), 102.
[19] Szcześniak, A., Stolarski, A.: Dynamic Relaxation Method for Load Capacity Analysis of Reinforced Concrete Elements. Applied Sciences, 2018, 8(3), 396.
[20] Li, J. B., Gao, X., Fu, X. A., Wu, C., Lin, G.: A nonlinear crack model for concrete structure based on an extended scaled boundary finite element method. Applied Sciences, 2018, 8(7), 1067.
[21] Azarinfar, H., Aghaebrahimi, M. R. Design, Analysis and Fabrication of a Novel Transverse Flux Permanent Magnet Machine with Disk Rotor. Applied Sciences, 2017, 7(8), 860.
[22] Ścieszka, S., Żołnierz, M.: Wpływ cech konstrukcyjnych hamulca tarczowego maszyny wyciągowej na jego niestabilność termosprężystą. Część I. Budowa modelu MES i jego weryfikacja. Zagadnienia Eksploatacji Maszyn, 2007, 42.3: 111-124.
[23] Różyło, P., Gajewski, J., Nowakowski, P., Machrowska, A.: Zastosowanie sieci RBF w analizie pękania elementów maszyn. Logistyka, 2015, (3), 4172-4186.
[24] Jachimowicz, J., Wawrzyniak, A.: Zastosowanie MES w zagadnieniach kontaktu elementów maszyn. Prace Instytutu Podstaw Budowy Maszyn/Politechnika Warszawska, 1999, 69-108.
[25] Chichociński, A., Ładecki, B.: Analiza przyczyn powstawania pęknięć zmęczeniowych w konstrukcji bębna pędnego maszyny wyciągowej. Mechanics/AGH University of Science and Technology, 2005, 24: 166-172.
[26] Truty, G., Nycz, D., Ślązkiewicz, M.: Numeryczne obliczenia wytrzymałościowe stołu adaptacyjnego do prasy. Modelowanie Inżynierskie, 2017, 33.
[27] Selech, J., Romek, D., Ulbrich, D., Włodarczyk, K., Staszak, Ż., Marcinkiewicz, J., Zbonik, M.: Projekt maszyny do bezwykopowego układania węży drenarskich. W: XXII Międzynarodowa Szkoła komputerowego wspomagania projektowania, wytwarzania i eksploatacji, Wyd. WAT, 2018, 334-340.
[28] Lachowicz, M. B., Lachowicz, M. M. Właściwości użytkowe, projektowe i technologiczne stali konstrukcyjnych klasyfikowanych według obowiązujących norm i stosowanych w budowie maszyn //Górnictwo Odkrywkowe, 2013, 54.

[29] Marcinkiewicz J., Bieńczak A., Dembicki D., Dudziński P., Mac J., Szczepaniak J. Strength analysis of insulated body with the use of FEM // Journal of Research and Applications in Agricultural Engineering, 60(1). 2015
[30] Marcinkiewicz J., Selech J., Staszak Ż., Gierz Ł., Ulbrich D., Romek D. DEM simulation research of selected sowing unit elements used in a mechanical seeding drill // MATEC Web of Conferences, Vol. 254, 2019, p. 02021
[31] Niesłony P., Grzesik W. Modelowanie procesu i operacji skrawania metodą elementów skończonych (MES) Cz. I. Podstawy i programy symulacyjne //Mechanik, 86(10), 2013, 825-826.
[32] Selech J., Ulbrich D., Włodarczyk K., Kowalczyk J., Adamkiewicz J. The prototype of stream amplifier used in transport of polydisperse medium //Procedia engineering, 2017, 192, P. 777–781.
[33] Kilikevičius, A., Bačinskas D., Selech J., Matijošius, J., Kilikevičien K., Vainorius D., Ulbrich D., Romek D. The influence of different loads on the footbridge dynamic parameters //Symmetry, 12 (4), 2020, 657.
[34] Pieniak D, Walczak A, Oszus M, Przystupa K, KamockaBronisz R, Piec R. Influence of thermal shocks on residual static strength, impact strength and elasticity of polymercomposite materials used in firefighting helmets //Materials, 2022,15(1), 57.
[35] Selech J., Ulbrich D., Kęska W., Staszak Ż., Marcinkiewicz J., Romek D., Rogoziński P., Design of a cultivator mounted on a tractor with a power of up to 20 kW //MATEC Web Conferences 254, 1-7, (2019).
[36] Durczak K., Selech J., Ekielski A., Żelaziński T., Waleński M., Witaszek K., Using the Kaplan–Meier Estimator to Assess the Reliability of Agricultural Machinery //Agronomy *12*, 2022, 1364.
[37] Domagała I., Gil L., Firlej M., Pieniak D., Selech J., Romek D., Biedziak B., Statistical Comparison of the Hardness and Scratch-Resistance of the PMMA Polymers Used in Orthodontic Appliances //Adv. Sci. Technol. Eng. Syst. J, 2020, 14, 250–261.
[38] Przystupa K., Chornodolskyy Y.M., Selech J., Karnaushenko V.O., Demkiv T.M., Kochan O., Syrotyuk S.V., Voloshinovskii A.S., The Influence of Halide Ion Substitution on Energy Structure and Luminescence Efficiency in CeBr2I and CeBrI2 Crystals //Materials, 2023, 16, 5085.
[39] Przystupa K., Beshley M., Hordiichuk-Bublivska O., Kyryk M., Beshley H., Pyrih J., Selech J., Distributed Singular Value Decomposition Method for Fast Data Processing in Recommendation Systems // Energies, 2021, 14, 2284.
[40] Kilikevičius A., Bačinskas D., Selech J., Matijošius J., Kilikevičienė K., Vainorius D., Ulbrich D., Romek D., The Influence of Different Loads on the Footbridge Dynamic Parameters // Symmetry, 2020, 12, 657.
[41] Paczkowska M., Selech J., Microstructure and Soil Wear Resistance of a Grey Cast Iron Alloy Reinforced with Ni and Cr Laser Coatings //Materials 2022, 15, 3153.
[42] Durczak K., Selech J., The Quantification of Operational Reliability of Agricultural Tractors with the Competing Risks Method, Tehnički vjesnik, vol. 29, no. 2, 2022, P. 628-633.
[43] Warguła Ł., Wojtkowiak D., Kukla M., & Talaśka, K. Symmetric nature of stress distribution in the elastic-plastic range of Pinus L. pine wood samples determined experimentally and using the finite element method (FEM). Symmetry 2020, 13(1), 39.
[44] Warguła Ł., Wojtkowiak, D., Kukla M., Talaśka K.. Modelling the process of splitting wood and chipless cutting Pinus sylvestris L. wood in terms of designing the geometry of the tools and the driving force of the machine // European Journal of Wood and Wood Products 2023, 81(1), 223-237
[45] Warguła Ł., Lijewski P., Kukla M. Effects of Changing Drive Control Method of Idling Wood Size Reduction Machines on Fuel Consumption and Exhaust Emissions // Croatian Journal of Forest Engineering: Journal for Theory and Application of Forestry Engineering 2023, 44(1), P. 137-151.
[46] Warguła Ł., Wilczyński D., Wieczorek B., Palander T., Gierz L., Nati C., Sydor M. Characterizing Sawdust Fractional Composition from Oak Parquet Woodworking for Briquette and Pellet Production. Advances in Science and Technology //Research Journal, 2023, 17(5).
[47] Kaczmarzyk, P., Małozięć, D., Burdzy, T., Ziegler, B., Krawiec, P., Dziechciarz, A., & Warguła, Ł. Analysis of the air stream flow parameters generated by the positive pressure ventilator - full scale experiment and CFD simulation //Scientific Reports 2024, 14(1), 6852.

Information of the authors

Marcinkiewicz Jacek, msc. eng., assistant, Poznan University of Technology
e-mail: jacek.marcinkiewicz@put.poznan.pl

Spadło Mikołaj, PhD Eng., assistant professor, Poznan University of Technology
e-mail: mikolaj.sspadlo@put.poznan.pl

Staszak Żaneta, PhD Eng., assistant professor, Poznan University of Technology
e-mail: staszak.zaneta@put.poznan.pl